Bull. Mater. Sci., Vol. 34, No. 4, July 2011, pp. 907–914. © Indian Academy of Sciences.

Structural, dielectric and electrical properties of $CaBa_4SmTi_3Nb_7O_{30}$ ferroelectric ceramic

PRASUN GANGULY and A K JHA*

Thin Film and Materials Science Laboratory, Department of Applied Physics,
Delhi Technological University (Formerly Delhi College of Engineering), Bawana Road, Delhi 110 042, India

MS received 21 January 2010; revised 12 April 2010

Abstract. The polycrystalline sample of $CaBa_4SmTi_3Nb_7O_{30}$, a member of tungsten bronze family, was prepared by solid-state reaction method. X-ray diffraction analysis shows the formation of single-phase compound with an orthorhombic structure at room temperature. Scanning electron micrograph of the material shows uniform distribution of grains. Detailed studies of dielectric properties of the compound as a function of temperature at different frequencies suggest that the compound has a dielectric anomaly of ferroelectric to paraelectric type at 198°C, and exhibits non-relaxor kind of diffuse phase transition. The ferroelectric nature of the compound has been confirmed by recording polarization–electric field hysteresis loop. Piezoelectric and pyroelectric studies of the compound have been discussed in this paper. Electrical properties of the material have been analyzed using complex impedance technique. The Nyquist plots manifest the contribution of grain boundaries (at higher temperature), in addition to granular contribution (at all temperatures) to the overall impedance. The temperature dependence of dc conductivity suggests that the compound has negative temperature coefficient of resistance (NTCR) behaviour. The frequency dependence of ac conductivity is found to obey Jonscher's universal power law. The observed properties have been compared with calcium free $Ba_5SmTi_3Nb_7O_{30}$ compound.

Keywords. Ferroelectrics; solid-state reaction; X-ray diffraction; dielectric response; electrical properties.

1. Introduction

Tungsten-bronze (TB) ferroelectric oxides owing to their structural flexibility have received considerable attention and have been found to be useful for device applications such as actuators, transducers, capacitors, electro-optic, ferroelectric random access memories, etc (Newnham *et al* 1980; Xu *et al* 1991; Wakiya *et al* 1999; Bhattacharya and Ravichandran 2003; Szwagierczak and Kulawik 2004). The TB type structure consists of a complex array of distorted BO_6 octahedral sharing corners in such a way that three different types of interstices (A, B and C) are available for cation occupation in the general formula $[(A_1)_4(A_2)_2(C)_4][(B_1)_2(B_2)_8]O_{30}$ (Jasmieson *et al* 1968). In this formula, A_1 and A_2 sites are usually filled by divalent or trivalent cations, B_1 and B_2 sites by tetravalent or pentavalent cations and C site being small, often remains empty giving the general formula $A_6B_{10}O_{30}$. There is a scope for substitution by variety of cations at many interstitial sites (i.e. A_1, A_2, B_1, B_2) that can tailor the physical properties of the compound for various device applications. A number of rare earth based compounds including $Ba_5RTi_3Nb_7O_{30}$, $Ba_4R_2Ti_4Nb_6O_{30}$ and $Ba_3R_3Ti_5Nb_5O_{30}$ (R = Nd, Sm, Eu, Gd, Dy and Y) of this family have been studied in order to find out new TB niobate type of ceramics which show diffuse phase transition with transition temperature above the room temperature (Choudhary *et al* 1999; Palai *et al* 2001; Rao *et al* 2001; Ganguly *et al* 2009a). Earlier the authors have done detailed structural and electrical studies on $Ba_5SmTi_3Nb_7O_{30}$ compound (Ganguly *et al* 2008, 2009b). The present work aims to understand the effect of partial substitution of calcium in $Ba_5SmTi_3Nb_7O_{30}$ (BSTN) compound. This paper summarizes the results of an extensive study made on the structural, dielectric and electrical properties of $CaBa_4SmTi_3Nb_7O_{30}$ (CBSTN) compound.

2. Experimental procedure

The polycrystalline sample of CBSTN was prepared by solid-state reaction technique by taking high purity $CaCO_3$, $BaCO_3$, TiO_2, Nb_2O_5 (all from M/s Aldrich, USA) and Sm_2O_3 (M/s Alfa Aesar, USA) in their stoichiometric proportions. The materials were thoroughly ground in an agate mortar and passed through a sieve of extremely fine mesh size. This powder mixture was then calcined at 1100°C for 20 h in an alumina crucible. The calcined mixture was ground, passed through

*Author for correspondence (dr_jha_ak@yahoo.co.in)

the sieve again. The mixture was then admixed with 5 wt.% polyvinyl alcohol (M/s Aldrich, USA) as a binder and then pressed at 300 MPa into a disk shaped pellet. This pellet was then sintered at 1300°C for 10 h. This is the optimized sintering condition found from extensive studies reported elsewhere (Ganguly *et al* 2009a).

X-ray diffractogram of the sintered pellet was recorded using Bruker diffractometer (model D8 Advance) in the range $10° < 2\theta < 70°$ with CuK_α radiation (λ = 1·5405 Å) with a scanning rate of 1°/min. The granular morphology of the sample was investigated using Scanning Electron Microscope (Jeol, JSM-840), operated at 20 kV. The sintered pellet was polished and silver pasted on both sides and cured at 325°C for 1 h. The dielectric and impedance measurements were carried out using LCR meter (Agilent 4284A) operating at oscillation amplitude of 1 V. The impedance measurements have been carried out in the temperature range of 325–400°C at an interval of 25°C and frequencies ranging from 20 Hz to 500 kHz. The polarization–electric field (P–E) hysteresis measurement was done using an automatic P–E loop tracer based on Sawyer–Tower circuit. The measurement of the pyroelectric coefficient was performed using the Byer-Roundy technique (Roundy and Byer 1973). The samples were first poled at 12 kV/cm at an elevated temperature (~ 140°C) for 2 h in silicon oil. The poled samples were then placed in a programmable furnace, and the temperature was increased at a rate of 2°C/min. The current generated in the specimen was measured using a high precision electrometer (Keithley 6517A). Piezoelectric co-efficient (d_{33}) was measured using a piezometer system (PiezoTest PM300) on the poled sample.

3. Results and discussion

3.1 *Structural and microstructural analysis*

Room temperature X-ray diffraction pattern of CBSTN is shown in figure 1, which reveals the formation of single–phase compound. The lattice parameters were calculated using the observed interplanar spacing, d-values, obtained from the diffractogram and refined using the least square refinement method by a computer program package PowderX (Dong 1999). The lattice parameters so obtained are: a = 6·3078 Å, b = 5·5914 Å, c = 6·8250 Å. The peaks were indexed using the observed d-values and the calculated lattice parameters. From these, it is found that CBSTN has an orthorhombic TB-type structure.

The SEM micrographs, both secondary electron (SE) and back-scattered electron (BSE), of CBSTN sample is shown in figure 1 (inset). It is found that with calcium addition the average grain size increases and the shape of the grain changes from spherical to cylindrical. Similar shape change of grains on addition of calcium has been reported earlier also (Das *et al* 2004).

3.2 *Dielectric studies*

The dielectric constant (ε'_r)of the specimen has been measured from room temperature to 300°C at frequencies of 1 kHz, 10 kHz and 100 kHz and is shown in figure 2(a). It is found that the compound has a dielectric anomaly at 198°C (the Curie temperature T_c) indicating the occurrence of ferroelectric–paraelectric phase transition. It is also observed that the compound has the same T_c at all the above mentioned frequencies, indicating that the compound does not have a relaxor behaviour (Das *et al* 2008). It is observed that the dielectric constant decreases on addition of calcium. This is possibly due to the decrease in the net polarization of the compounds with substitution of calcium as the ionic polarizability, α_I of Ca is 3·16 $Å^3$ compared to that of Ba 6·40 $Å^3$ (Shannon 1993). However, T_c increases from 170°C (in BSTN) to 198°C (in CBSTN) which could be attributed to the reduced value of the tolerance factor due to the partial substitution of smaller cation Ca at Ba-site (Das *et al* 2004).

The dielectric peak is broadened indicating the existence of diffuse phase transition. The diffusivity constant or degree of disorderness (γ) was calculated using the formula (Pilgrim *et al* 1990)

$$\ln(1/\varepsilon'_r - 1/\varepsilon'_{rmax}) = \gamma \ln(T - T_c) + \text{constant}. \quad (1)$$

The value of γ at 100 kHz calculated from the slope of linearly fitted curve with (1) is shown in figure 2(a) (inset). It is between 1 (obeying Curie–Weiss law) and 2 (for completely disordered system) indicating a diffuse kind of phase transition as indeed observed. The partial substitution of Ca at the Ba-site in the compound results in the reduction of the diffusivity constant (γ) indicating the compound becomes more ordered (Sen and Choudhary 2004).

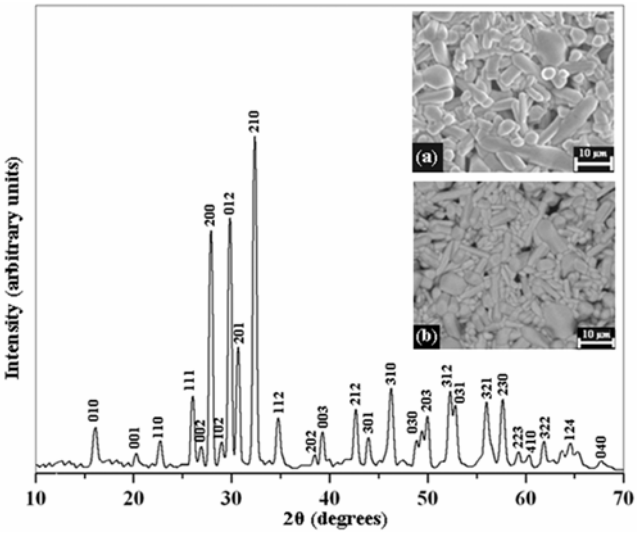

Figure 1. X-Ray diffraction pattern and SEM micrograph (inset) (**a**) SE and (**b**) BSE of $CaBa_4SmTi_3Nb_7O_{30}$ compound.

Figure 2(b) shows the temperature variation of dielectric loss (tanδ) from room temperature to 300°C at the frequencies of 1 kHz, 10 kHz and 100 kHz. At all the above mentioned frequencies, the variation of dielectric loss with temperature shows that the loss has smaller values at lower temperatures but at higher temperatures it increases sharply. This sharp increase of tan δ in high temperature region may be attributed to the increased mobility of space charges at higher temperatures arising from the defects or vacancies (like oxygen vacancies) in the sample (Behera *et al* 2006).

3.3 *Ferroelectric studies*

To confirm the ferroelectric nature and the Curie-temperature (T_c) of the studied compound, temperature dependent *P–E* hysteresis loops were recorded at a frequency of 100 Hz and are shown in figure 3. The existence of hysteresis loop confirms the ferroelectric nature of the compound. The remanent polarization ($2P_r$) value at room temperature is 2·5 μC/cm^2 and the coercive field ($2E_c$) is 36·7 kV/cm. It can be seen that the remanent polarization ($2P_r$) value decreases with increasing temperature and finally becomes zero around the transition temperature (T_c) i.e. 198°C. On addition of calcium, $2P_r$ value increases which could be correlated to the pronounced structural distortion arising due to the partial substitution of smaller cation Ca at Ba-site (Das *et al* 2004).

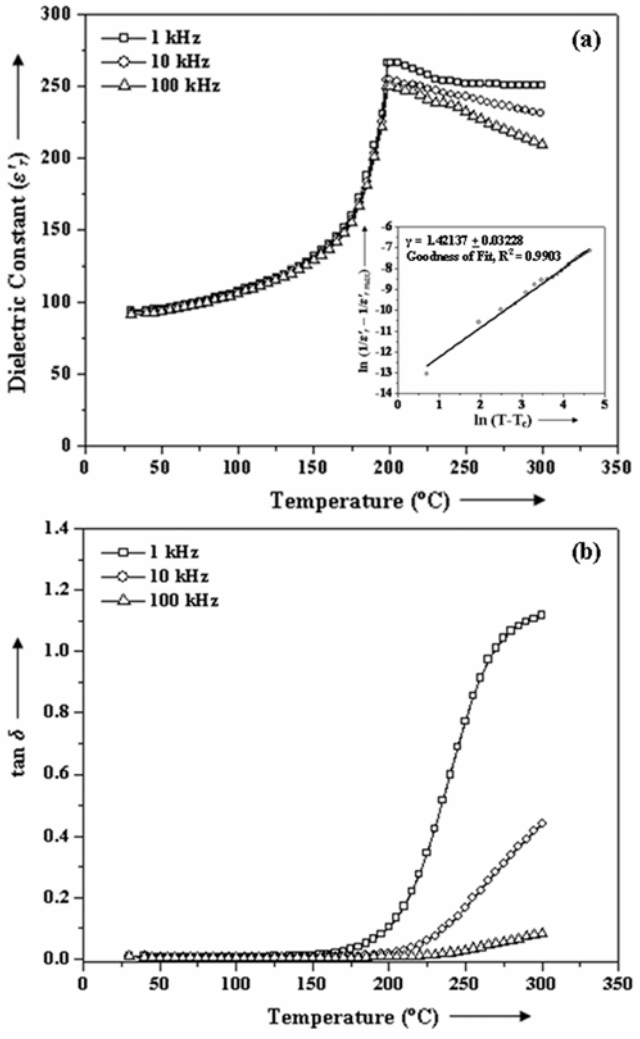

Figure 2. (**a**) Variation of dielectric constant (ε'_r) with temperature at 1 kHz, 10 kHz, 100 kHz frequencies and variation of $\ln(1/\varepsilon'_r - 1/\varepsilon'_{rmax})$ with $\ln(T - T_c)$ at 100 kHz (inset). (**b**) Variation of dielectric loss (tan δ) with temperature at 1 kHz, 10 kHz, 100 kHz frequencies of $CaBa_4SmTi_3Nb_7O_{30}$ compound.

3.4 *Pyroelectric and piezoelectric studies*

The temperature variation of pyroelectric coefficient of CBSTN compound synthesized is shown in figure 4. The pyroelectric coefficient (P_T) was calculated using the relation (Lang 1974)

$$P_T = \frac{P_I}{A\left(\frac{dT}{dt}\right)}, \tag{2}$$

where P_I is the pyroelectric current, A the area of the conducting surface of the sample and dT/dt is the rate of change of temperature. The pyroelectric current as well as pyroelectric coefficient passes through a peak at a temperature (160°C) lower than the ferroelectric transition temperature (T_c). The maximum pyroelectric coefficient at this temperature is 53·1 nCcm^{-2}°C^{-1} which is lesser than that obtained in BSTN compound (Ganguly *et al* 2009a). The pyroelectric current is generated due to the change in spontaneous polarization with temperature (Uchino 2000). It is known that in diffuse phase transition, the rate of change of spontaneous polarization with temperature is maximum at a temperature below T_c (Uchino 2000), which is confirmed in the present work.

The d_{33} value in $CaBa_4SmTi_3Nb_7O_{30}$ compound is 5 pC/N which confirms the piezoelectric behaviour of the compound.

3.5 *Impedance studies*

Complex impedance spectroscopy (CIS) technique (MacDonald 2005) is an important tool to investigate the electrical properties of polycrystalline materials. It helps to separate the electrical resistivity due to grains and grain boundaries, and provides the true picture of the electrical properties of a material. This technique also shows the response of a system to a sinusoidal perturbation and gives impedance as a function of frequency. The resultant response (when plotted in a complex plane)

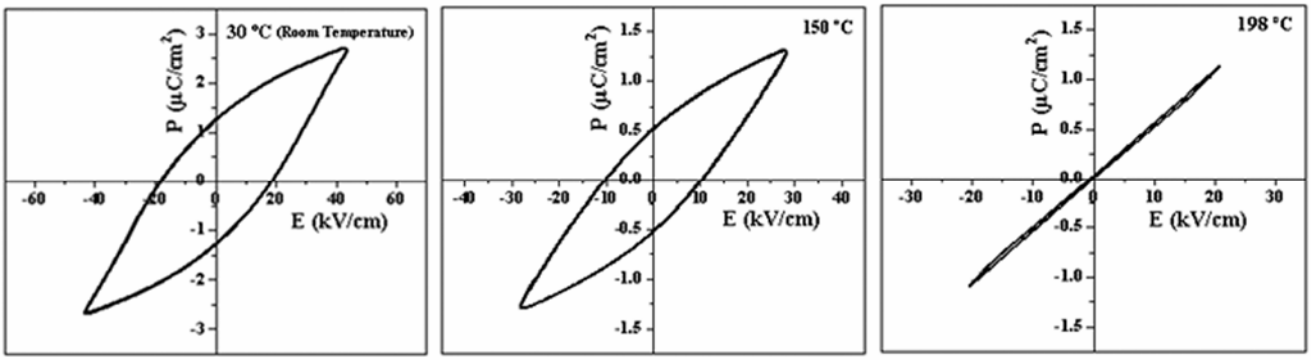

Figure 3. Temperature variation of *P–E* hysteresis loop in $CaBa_4SmTi_3Nb_7O_{30}$ compound.

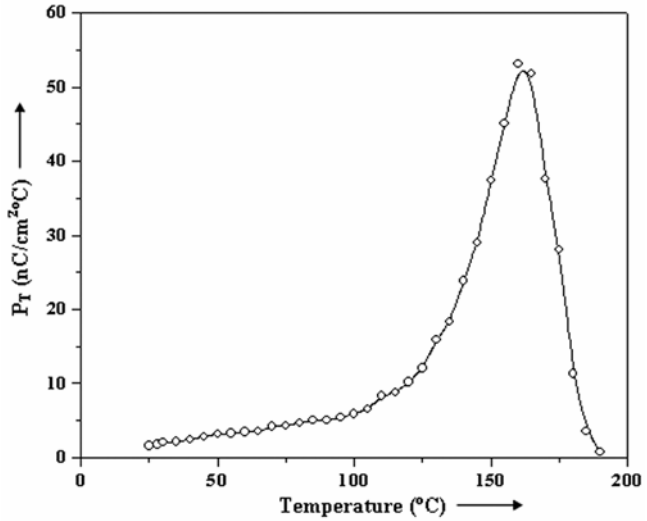

Figure 4. Temperature variation of pyroelectric coefficient (P_T) in $CaBa_4SmTi_3Nb_7O_{30}$ compound.

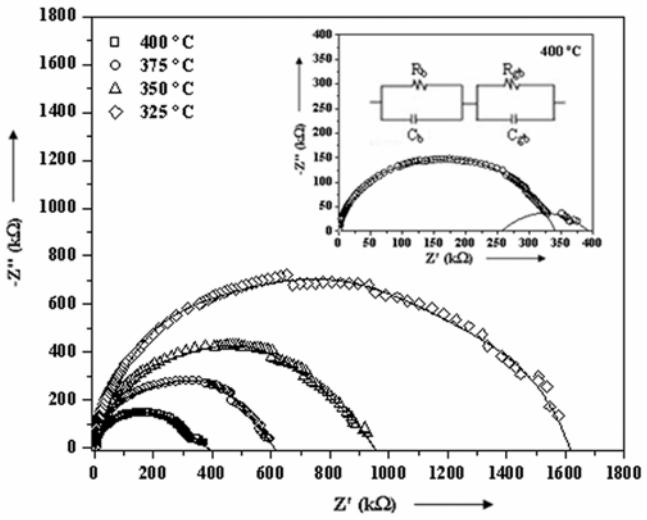

Figure 5. Complex impedance spectrum (Nyquist plots) of $CaBa_4SmTi_3Nb_7O_{30}$ at different temperatures.

appears in the form of a succession of semicircles representing electrical phenomena inside the material due to the bulk, grain boundary and interface. A polycrystalline specimen usually shows both grain and grain boundary effects with different time constants leading to two successive semicircles (Behera *et al* 2007).

The plot of real part (Z') versus imaginary part (Z'') of impedance (Nyquist or Cole-Cole plots) at different temperatures (325°C, 350°C, 375°C and 400°C) taken over a wide frequency range (20 Hz to 500 kHz) is shown in figure 5. All the semicircles exhibit some depression instead of a semicircle centered on the real axis. This behaviour is indicative of non-Debye type of relaxation and it also manifests that there is a distribution of relaxation time instead of a single relaxation time in the material (Sen *et al* 2007). The values of bulk resistance (R_b) at different temperatures have been obtained from the intercept of the semicircular arcs on the real axis (Z') and are given in table 1. It is observed that R_b decreases with the rise in temperature. This manifests that the negative temperature coefficient of resistance (NTCR) behaviour is maintained even after partial substitution of calcium in BSTN compound. However, the presence of two semicircles at higher temperature (i.e. 400°C) indicates the presence of both grain (bulk property) and grain boundary effects which can be represented by two parallel RC circuits connected in series as shown in figure 5 (inset). The high frequency semicircle corresponds to the bulk contribution, and the low frequency semicircle corresponds to the grain boundary effect (Behera *et al* 2007). The second intercept of each semicircle on real (Z')-axis gives the respective value of resistance (e.g. R_b and R_{gb}). The semicircles in the impedance spectrum have a characteristic peak occurring at a unique relaxation frequency ($\omega_r = 2\pi f_r$). It can be expressed as

$$\omega_r RC = \omega_r \tau = 1.$$

Therefore,

$$f_r = \frac{1}{2\pi\tau} = \frac{1}{2\pi RC}, \tag{3}$$

where τ is relaxation time. The corresponding capacitances (C_b and C_{gb}) due to the grain and grain boundary effect can be calculated using this relation. The values of

Table 1. Bulk and grain boundary resistances and capacitances of $CaBa_4SmTi_3Nb_7O_{30}$ compound.

Temperature (°C)	R_b (kΩ)	C_b (pF)	R_{gb} (kΩ)	C_{gb} (pF)
325	1621	182	–	–
350	951	220	–	–
375	619	222	–	–
400	340	224	53	2503

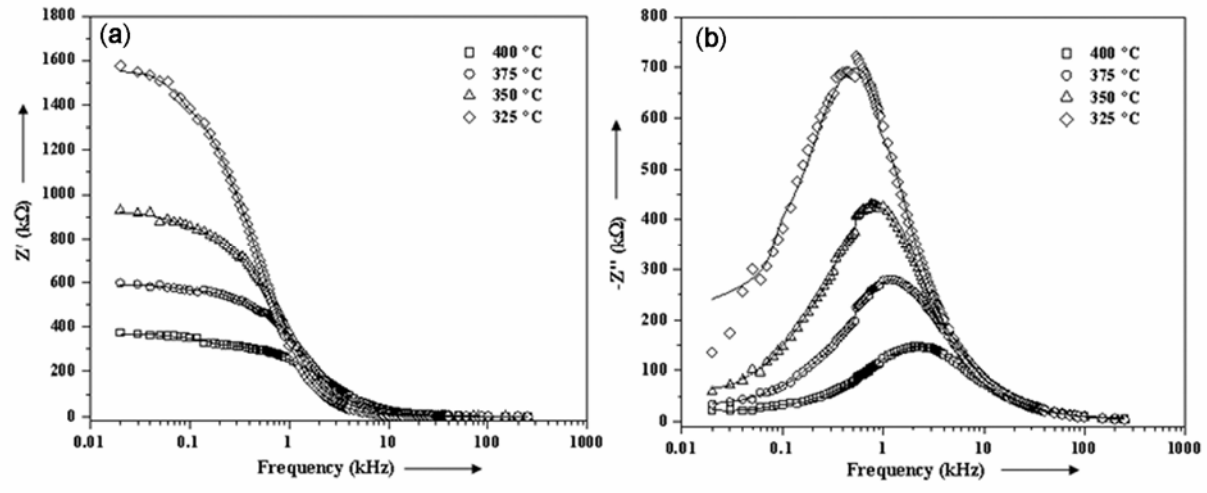

Figure 6. (**a**) Variation of real part of impedance (Z') with frequency. (**b**) Variation of imaginary part of impedance (Z'') with frequency.

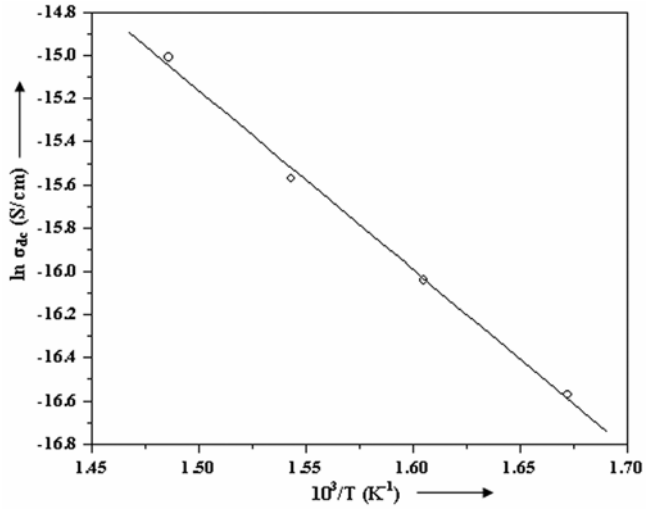

Figure 7. Variation of dc conductivity ($\ln\sigma_{d.c.}$) with inverse of temperature (10^3/T).

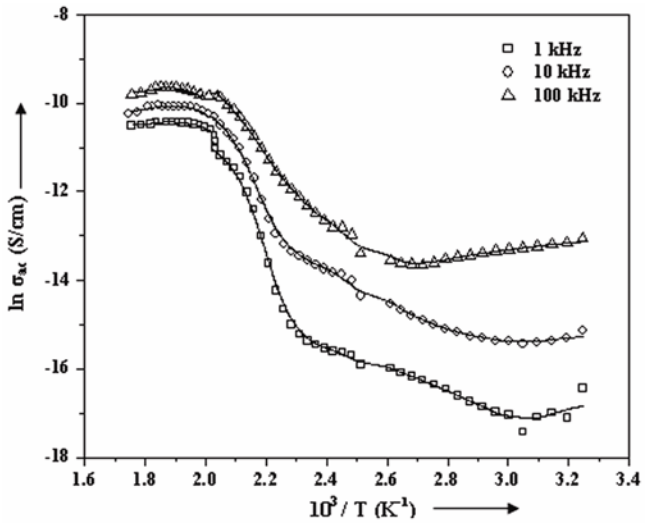

Figure 8. Variation of ac conductivity ($\ln\sigma_{a.c.}$) with inverse of temperature (10^3/T) at 1 kHz, 10 kHz, 100 kHz frequencies.

R_b, R_{gb}, C_b and C_{gb} obtained from Cole-Cole plots at different temperatures are listed in table 1.

Figure 6(a) shows the variation of Z' with frequency at different measuring temperatures. It is observed that the value of Z' decreases with increase of both frequency and temperature which indicates that the conductivity is increasing with rise in temperature (Mahajan *et al* 2009). This shows the presence of space charge (oxygen vacancies) conduction at low frequencies; however, at high frequencies, for all the temperatures, the values of Z' merge and is independent of frequency which indicates

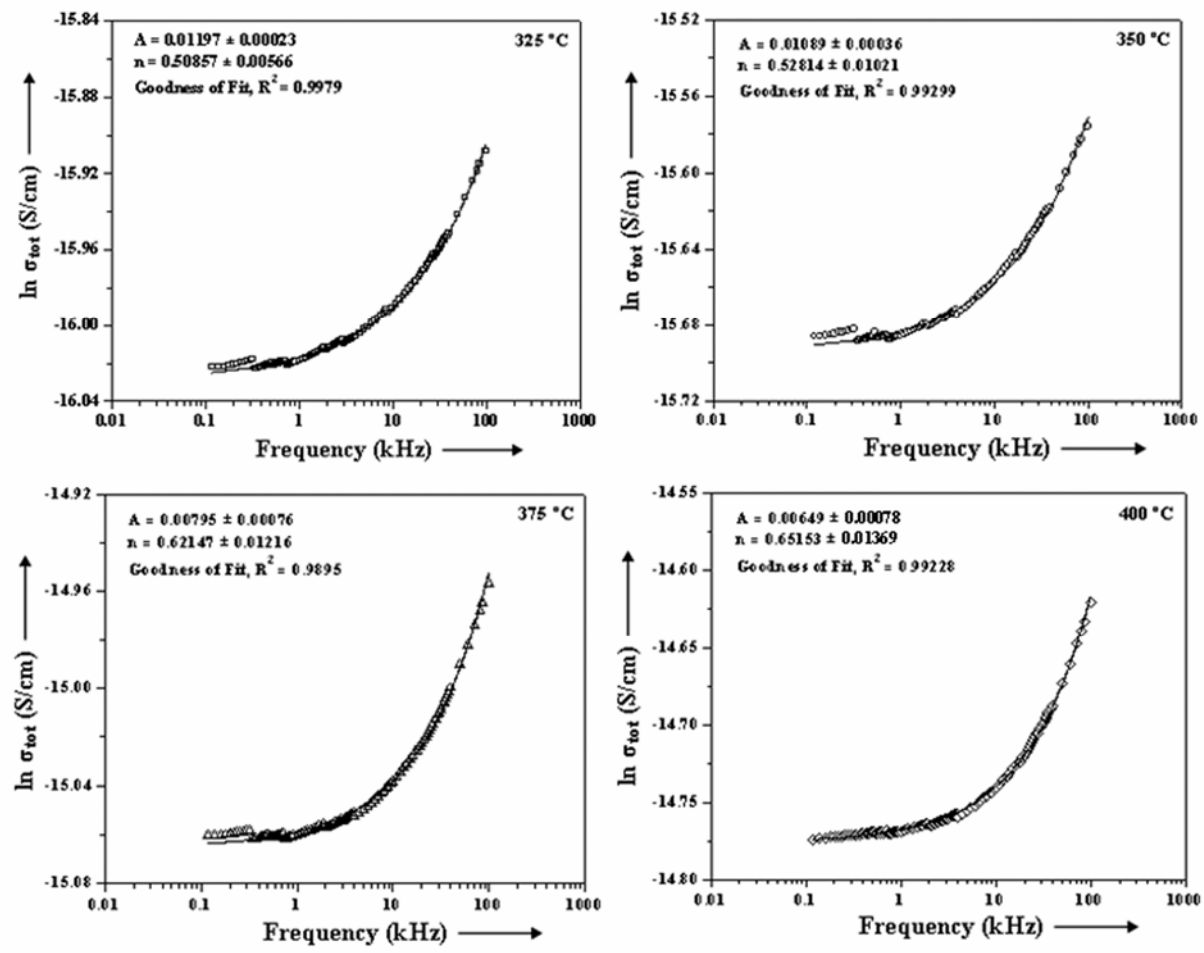

Figure 9. Variation of total conductivity of $CaBa_4SmTi_3Nb_7O_{30}$ as a function of frequency at different temperatures.

the inability of space charges to follow the high frequency fields (Plocharski and Wieczoreck 1988).

Figure 6(b) shows the variation of Z'' with frequency at various temperatures. The plots show that the Z'' values attain a peak (Z''_{maax}) at all the temperatures and the magnitude of Z''_{maax} decreases with increasing measuring temperature. The value of Z''_{maax} shifts to higher frequencies with increasing temperature, indicating the relaxation in the system. The peak broadening on increasing temperature, suggests the presence of temperature dependent relaxation processes in the compound (Behera *et al* 2008). The contribution towards relaxation process is possibly due to electrons at low temperature and defects/vacancies at higher temperature (Das *et al* 2008).

3.6 *Conductivity studies*

The d.c. (bulk) conductivity, $\sigma_{d.c.}$, of the sample has been evaluated from the impedance spectrum using the relation

$$\sigma_{d.c.} = \frac{t}{R_b A}, \tag{4}$$

where R_b is the bulk resistance, t the thickness and A the surface area of the sample. Figure 7 shows the variation of $\ln\sigma_{d.c.}$ with $10^3/T$. It is observed to increase with increasing temperature further confirming the NTCR behaviour. The nature of variation is linear and follows the Arrhenius relationship

$$\sigma_{d.c.} = \sigma_0 \exp\left(\frac{-E_a}{k_B T}\right), \tag{5}$$

where E_a is the activation energy of conduction and T is the absolute temperature. The value of activation energy (E_a) as calculated from the slope of $\ln\sigma_{d.c.}$ vs $10^3/T$ curve is 0·67 eV.

The a.c. conductivity ($\sigma_{a.c.}$) of the sample has been calculated using the relation (Kingery 1976)

$$\sigma_{a.c.} = \omega\varepsilon' r\varepsilon_0 \tan\delta, \tag{6}$$

where ω is the angular frequency, ε_o is the free space permittivity and k_B is the Boltzmann constant. Figure 8 shows the variation of a.c. conductivity as a function of temperature at different frequencies. At low temperatures, the ac conductivity is almost independent of temperature but shows different values at various frequencies indicating that main contribution to the conductivity results from the presence of space charges. As the temperature increases, the conductivity increases and subsequently all the curves come closer at high temperatures. Different slope changes appear in different regions of temperature, indicating the involvement of multiple activation processes with different energies. The value of activation energy (E_a) of the compound in the ferroelectric phase at 1 kHz, 10 kHz and 100 kHz is 0·32 eV, 0·28 eV and 0·19 eV respectively.

The frequency dependence of electric conductivity can be represented by an equation proposed by Jonscher (1977)

$$\sigma_{tot} = \sigma_{dc} + \sigma_{a.c.}(\omega) = \sigma_o + A\omega_n, \quad (7)$$

where $\sigma_{d.c.}$ (or σ_0) is the dc conductivity due to excitation of electron from a localized state to the conduction band, and $A\omega^n$ is the ac conductivity due to the dispersion phenomena occurring in the material. A is a temperature dependent constant and n is the power law exponent which generally varies between 0 and 1 depending on temperature. The exponent n represents the degree of interaction between mobile ions with the lattice around them and the prefactor A determines the strength of polarizability (Karthik and Varma 2006). Figure 9 shows the variation of total conductivity as a function of frequency at different measuring temperatures. CBSTN compound is observed to obey the Jonscher's equation (7) and the Jonscher's fitting results are given in the inset of figure 9 for each measuring temperature. It is found that parameter A decreases and n increases with temperature. Also, it can be seen that as frequency increases there is switching from the frequency independent σ_{dc} to frequency dependent $\sigma_{a.c.}(\omega)$ region and the frequency at which this switching occurs is known as the hopping frequency ω_p. This indicates the onset of the conductivity relaxation phenomenon and the translation from the long range to the short range localized hopping of charges (Sen *et al* 2007).

4. Conclusions

The synthesized $CaBa_4SmTi_3Nb_7O_{30}$ compound is in single phase having an orthorhombic tungsten-bronze crystal structure. SEM micrograph shows distribution of cylindrical grains throughout the specimen. The compound shows a diffuse type of ferroelectric – paraelectric phase transition having non-relaxor behaviour with a T_c of 198°C. The room temperature P–E hysteresis loop with $2P_r$ value of 2·5 μC/cm^2 and the pyroelectric coefficients observed at different temperatures confirm the ferroelectric nature of the compound. Complex impedance analysis suggests dielectric relaxation to be polydispersive non-Debye type with a temperature dependent behaviour. The compound shows negative temperature coefficient of resistance (NTCR) behaviour.

Acknowledgement

One of the authors (PG) is grateful to Council of Scientific and Industrial Research (CSIR), New Delhi, India for the award of Senior Research Fellowship.

References

Behera B, Nayak P and Choudhary R N P 2006 *Mat. Chem. Phys.* **100** 138

Behera B, Nayak P and Choudhary R N P 2007 *J. Alloys Comp.* **436** 226

Behera B, Nayak P and Choudhary R N P 2008 *Mat. Res. Bull.* **43** 401

Bhattacharya K and Ravichandran G 2003 *Acta Mater.* **51** 5941

Choudhary R N P, Shannigrahi S R and Singh A K 1999 *Bull. Mater. Sci.* **22** 975

Das R R, Bhattacharya P, Pérez W, Katiyar R S 2004 *Ceram. Int.* **30** 1175

Das P R, Choudhary R N P and Samantray B K 2008 *J. Alloys Comp.* **448** 32

Dong C 1999 *J. Appl. Crystallogr.* **32** 838

Ganguly P, Jha A K and Deori K L 2008 *Solid State Commun.* **146** 472

Ganguly P, Jha A K and Deori K L 2009a *J. Alloys & Comp.* **484** 40

Ganguly P, Jha A K and Deori K L 2009b *J. Electroceram.* **22** 257

Jasmieson P B, Abrahams S C and Bernstein L 1968 *J. Chem. Phys.* **48** 5048

Jonscher A K 1977 *Nature* **267** 673

Karthik C and Varma K B R 2006 *J. Phys. Chem. Solids* **67** 2437

Kingery W D 1976 *Introduction to ceramics* (eds) W D Kingery, H K Bowen and D R Uhlmann (New York: John Wiley and Sons Inc.) 2nd edn

Lang S B 1974 *Source book of pyroelectricity* (New York: Gordan and Breach Science Publishers)

MacDonald J R 2005 *Impedance spectroscopy theory, experiment and applications* (eds) E Barsoukov and J R Macdonald (New Jersey: John Wiley & Sons Inc.) 2nd edn

Mahajan S, Thakur O P, Bhattacharya D K and Sreenivas K 2009 *J. Am. Ceram. Soc.* **92** 416

Newnham R E, Bowen L J, Klicker K A and Cross L E 1980 *Mater. Eng.* **2** 93

Palai R, Choudhary R N P and Tewari H S 2001 *J. Phys. Chem. Solids* **62** 695

Pilgrim S M, Sutherland A E and Winzer S R 1990 *J. Am. Ceram. Soc.* **73** 3122

Plocharski J and Wieczoreck W 1988 *Solid State Ionics* **28–30** 979
Rao P R, Ghosh S K and Koshy P 2001 *J. Mater. Sci.: Mater. Electron.* **12** 729
Roundy C B and Byer R L 1973 *J. Appl. Phys.* **44** 929
Sen S and Choudhary R N P 2004 *Mater. Lett.* **58** 661
Sen S, Choudhary R N P and Pramanik P 2007 *Phys.* **B387** 56
Shannon R D 1993 *J. Appl. Phys.* **73** 348
Szwagierczak D and Kulawik J 2004 *J. Eur. Ceram. Soc.* **24** 1979
Uchino K 2000 *Ferroelectric devices* (New York: Marcel Dekker Inc.)
Wakiya N, Wang J K, Saiki A, Shinozaki K and Mizutani N 1999 *J. Eur. Ceram. Soc.* **19** 1071
Xu Y, Chen C J, Xu R and Mackenzie J D 1991 *Phys. Rev.* **B44** 35